

Modulation effect in the differential and total rate for supersymmetric dark matter detection

J. D. Vergados

Theoretical Physics Section, University of Ioannina, GR-45110, Greece

(Received 30 January 1998; published 5 October 1998)

The modulation effect in the direct detection of supersymmetric cold dark matter (CDM) particles is investigated. A variety of nuclear targets (light, intermediate and heavy) are considered, taking into account the nuclear form factor effects and detector energy thresholds. It is shown that the nuclear form factor tends to decrease the modulation effect in the total event rate below its typical value of 5%. In spite of this, however, in some subregions of phase space, the modulation effect can become much larger, $h \leq 25\%$. It also becomes more pronounced in the differential event rate in some domains of the energy transfer. These effects may be exploited to discriminate against background. [S0556-2821(98)05918-9]

PACS number(s): 95.35.+d, 14.80.Ly

I. INTRODUCTION

In this work we will study the differential modulation effect of the event rate for detecting supersymmetric dark matter, i.e. its variation with respect to the energy transferred to the nucleus, due to Earth's motion.

There is now ample evidence that most of the matter of the Universe is non-luminous, i.e. dark [1], and is composed of two components. One is the hot dark matter (HDM) component consisting of particles which were relativistic at freeze out, while the other is cold dark matter (CDM) composed of particles which were non-relativistic. There are many arguments supporting the fact that CDM is at least 60% [2]. There are two interesting cold dark matter candidates: (i) massive compact halo objects (MACHO's) and (ii) exotic weakly interacting massive particles (WIMP's). Since there are indications that the MACHO's cannot exceed 40% of the CDM component [1,3], there is room for an exotic candidate. The most natural one is associated with supersymmetry, i.e. the lightest supersymmetric particle (LSP).

The most interesting possibility to directly detect the LSP [1,4] is via the recoiling of a nucleus (A, Z) in the process:

$$\chi + (A, Z) \rightarrow \chi + (A, Z)^* \quad (1)$$

(χ denotes the LSP). In the above process only the elastic channel is of practical interest, since either the energy of the LSP is too low to excite the nucleus or the cross-section is too low to be measurable. In computing the event rate for the above process one proceeds with the following steps:

(1) Write down the effective Lagrangian at the elementary particle (quark) level in the framework of supersymmetry as described in Refs. [1,4].

(2) Go from the quark to the nucleon level using an appropriate quark model for the nucleon. Special attention must be paid to the scalar couplings, which dominate the coherent part of the cross section, and the isoscalar axial current, which strongly depends on the assumed quark model [4,6].

(3) Compute the relevant nuclear matrix elements [5,7–10] using as reliable as possible many body nuclear wave functions.

(4) Calculate the modulation of the event rate due to Earth's revolution around the Sun [5,11].

There are many popular targets [12–14] for LSP detection as e.g. ^{19}F , ^{23}Na , ^{27}Al , ^{29}Si , ^{40}Ca , $^{73,74}\text{Ge}$, ^{127}I , ^{207}Pb , etc.

In a previous paper [5] we computed the modulation effect h , i.e. the oscillation amplitude of the total event rate (see below for its precise definition), by convoluting with the LSP velocity distribution the event rate, which, among other things, depends upon the relative velocity of the LSP with respect to Earth. Assuming a Maxwell Boltzmann distribution [1] of velocities for the LSP, we found that h cannot exceed the value of 5% which corresponds to small momentum transfer. The actual value of h is quite a bit smaller especially for heavy nuclei and relatively heavy LSP's ($m_\chi \geq 50$ GeV). It is known [5,12] that, in some cases, the quantity h may become negative, suggesting cancellations between the bins that correspond to small and those which correspond to relatively large energy transfers. It is thus possible that in some energy bins the modulation effect can be larger than the value of h quoted above.

The event rate depends on many parameters [4], since there exist many contributions to the above process. The most dominant appears to be the coherent contribution, which arises out of the scalar coupling originating from Higgs boson exchange or squark exchange if there exists mixing between the L and R squark varieties. It can also arise from the time component of the vector current originating from s-quark and Z exchange. The latter is favored from the point of view of the couplings but it is suppressed kinematically by factors of $\beta^2 \sim 10^{-6}$ owing to the fact that the LSP is a Majorana particle. Because of its different dependence on the LSP velocity, it yields a higher modulation effect. In addition to the coherent part, especially for light targets, when the target spin is non-zero, one must include the axial current (spin matrix element of the nucleus).

Our main purpose is, for typical light, intermediate and heavy nuclei and by taking into account the velocity dependence of the LSP-nucleus cross section, to calculate the following:

(i) The modulated and unmodulated parts of the total event rate for various detector energy thresholds.

(ii) The differential modulation effect H , i.e. the ratio of

the part of the differential event rate which depends on the position of Earth divided by that which does not (for its definition see below). If one considers each of the above mechanisms separately, H depends only on the LSP mass and the size of the nucleus. Knowledge of H may not be adequate, however, since one needs to know its value in the energy transfer regime where the event rate is the largest and hopefully measurable. One might also need the relative differential event rate, i.e. the ratio of the differential rate to the total rate. If one considers the above three mechanisms separately, the relative differential event rate is independent of the supersymmetry (SUSY) parameters or the structure of the nucleon. It depends on the nuclear structure only mildly through the form factors. So one can make quite accurate predictions which depend only on the nuclear size, the mass of the LSP and the low energy cutoff imposed by the detector.

II. EXPRESSIONS FOR THE RATE

As we have mentioned in the Introduction we only need calculate the fraction of the differential rate divided by the total rate which is independent of the parameters of supersymmetry. Thus we are not going to elaborate here further on these, but refer the reader to the literature [4,5,15,16]. For completeness we only give here expressions describing the effective Lagrangian obtained in first order via Higgs boson exchange, s-quark exchange and Z exchange. We will use a formalism which is familiar from the theory of weak interactions, i.e.

$$L_{eff} = -\frac{G_F}{\sqrt{2}} \{ (\bar{\chi}_1 \gamma^\lambda \chi_1) J_\lambda + (\bar{\chi}_1 \chi_1) J \} \quad (2)$$

where

$$J_\lambda = \bar{N} \gamma_\lambda (f_V^0 + f_V^1 \tau_3 + f_A^0 \gamma_5 + f_A^1 \gamma_5 \tau_3) N \quad (3)$$

and

$$J = \bar{N} (f_s^0 + f_s^1 \tau_3) N. \quad (4)$$

We have neglected the uninteresting pseudoscalar and tensor currents. Note that, due to the Majorana nature of the LSP, $\bar{\chi}_1 \gamma^\lambda \chi_1 = 0$ (identically). The parameters $f_V^0, f_V^1, f_A^0, f_A^1, f_S^0, f_S^1$ depend on the SUSY model employed. In SUSY models derived from minimal supergravity (SUGRA) the allowed parameter space is characterized at the grand unified theory (GUT) scale by five parameters, two universal mass parameters, one for the scalars, m_0 , and one for the gauginos, $m_{1/2}$, as well as the parameters $\tan \beta$, one of A_0 , or m_t^{pole} and the sign of μ [17]. Deviations from universality at the GUT scale have also been considered and found useful [18]. We will not elaborate further on this point since the above parameters involving universal masses have already been computed in some models [4,19] and effects resulting from deviations from universality will be published elsewhere [20] (see also Arnowitt and co-workers [18] and Bottino *et al.* [16]).

The invariant amplitude in the case of a non-relativistic LSP can be cast in the form [4]

$$|\mathcal{M}|^2 = \frac{E_f E_i - m_x^2 + \mathbf{p}_i \cdot \mathbf{p}_f}{m_x^2} |J_0|^2 + |\mathbf{J}|^2 + |J|^2 \approx \beta^2 |J_0|^2 + |\mathbf{J}|^2 + |J|^2 \quad (5)$$

where m_x is the LSP mass, $|J_0|$ and $|\mathbf{J}|$ indicate the matrix elements of the time and space components of the current J_λ of Eq. (3), respectively, and J represents the matrix element of the scalar current J of Eq. (4). Notice that $|J_0|^2$ is multiplied by β^2 (the suppression due to the Majorana nature of the LSP mentioned above). It is straightforward to show that

$$|J_0|^2 = A^2 |F(\mathbf{q}^2)|^2 \left(f_V^0 - f_V^1 \frac{A-2Z}{A} \right)^2 \quad (6)$$

$$J^2 = A^2 |F(\mathbf{q}^2)|^2 \left(f_S^0 - f_S^1 \frac{A-2Z}{A} \right)^2 \quad (7)$$

$$|\mathbf{J}|^2 = \frac{1}{2J_i + 1} |\langle J_i | [f_A^0 \boldsymbol{\Omega}_0(\mathbf{q}) + f_A^1 \boldsymbol{\Omega}_1(\mathbf{q})] | J_i \rangle|^2 \quad (8)$$

with $F(\mathbf{q}^2)$ the nuclear form factor and

$$\boldsymbol{\Omega}_0(\mathbf{q}) = \sum_{j=1}^A \sigma(j) e^{-i\mathbf{q} \cdot \mathbf{x}_j}, \quad \boldsymbol{\Omega}_1(\mathbf{q}) = \sum_{j=1}^A \sigma(j) \tau_3(j) e^{-i\mathbf{q} \cdot \mathbf{x}_j} \quad (9)$$

where $\sigma(j)$, $\tau_3(j)$, and \mathbf{x}_j are the spin, third component of isospin ($\tau_3 |p\rangle = |p\rangle$) and coordinate of the j th nucleon and \mathbf{q} is the momentum transferred to the nucleus.

The differential cross section in the laboratory frame takes the form [4]

$$\frac{d\sigma}{d\Omega} = \frac{\sigma_0}{\pi} \left(\frac{m_x}{m_N} \right)^2 \frac{1}{(1+\eta)^2} \xi \times \left\{ \beta^2 |J_0|^2 \left[1 - \frac{2\eta+1}{(1+\eta)^2} \xi^2 \right] + |\mathbf{J}|^2 + |J|^2 \right\} \quad (10)$$

where m_N is the proton mass, $\eta = m_x/m_N A$, $\xi = \hat{\mathbf{p}}_i \cdot \hat{\mathbf{q}} \geq 0$ (forward scattering) and

$$\sigma_0 = \frac{1}{2\pi} (G_F m_N)^2 \approx 0.77 \times 10^{-38} \text{ cm}^2. \quad (11)$$

The momentum transfer \mathbf{q} is given by

$$|\mathbf{q}| = q_0 \xi, \quad q_0 = \beta \frac{2m_x c}{1+\eta}. \quad (12)$$

Some values of q_0 (forward momentum transfer) for some

characteristic values of m_x and representative nuclear systems (light, medium and heavy) are given in Ref. [5]. It is clear from Eq. (12) that the momentum transfer can be

sizable for large m_x and heavy nuclei (η small).

Integrating the differential cross section, Eq. (10), with respect to the azimuthal angle we obtain

$$d\sigma(u_0, \xi) = \sigma_0 \left(\frac{m_x}{m_N} \right)^2 \frac{1}{(1+\eta)^2} \left[A^2 \left\{ \left[\beta^2 \left(f_V^0 - f_V^1 \frac{A-2Z}{A} \right)^2 + \left(f_S^0 - f_S^1 \frac{A-2Z}{A} \right)^2 \right] F^2(u_0 \xi^2) \right. \right. \\ \left. \left. - \frac{(\xi\beta)^2}{2} \frac{2\eta+1}{(1+\eta)^2} \left(f_V^0 - f_V^1 \frac{A-2Z}{A} \right)^2 F^2(u_0 \xi^2) \right\} + [f_A^0 \Omega_0(0)]^2 F_{00}(u_0 \xi^2) + 2 f_A^0 f_A^1 \Omega_0(0) \Omega_1(0) F_{01}(u_0 \xi^2) \right. \\ \left. + [f_A^1 \Omega_1(0)]^2 F_{11}(u_0 \xi^2) \right] 2\xi d\xi \quad (13)$$

where

$$F_{\rho\rho'}(u_0 \xi^2) = \sum_{\lambda, \kappa} \frac{\Omega_{\rho}^{(\lambda, \kappa)}(u_0 \xi^2)}{\Omega_{\rho}(0)} \frac{\Omega_{\rho'}^{(\lambda, \kappa)}(u_0 \xi^2)}{\Omega_{\rho'}(0)}, \quad \rho, \rho' = 0, 1. \quad (14)$$

The total cross section $\sigma(u_0, \beta)$, which has been studied previously (see e.g. [4,5]), can be cast in the form

$$\sigma = \sigma_0 \left(\frac{m_x}{m_N} \right)^2 \frac{1}{(1+\eta)^2} \left(A^2 \left\{ \left[\beta^2 \left(f_V^0 - f_V^1 \frac{A-2Z}{A} \right)^2 + \left(f_S^0 - f_S^1 \frac{A-2Z}{A} \right)^2 \right] I_0(u_0) \right. \right. \\ \left. \left. - \frac{\beta^2}{2} \frac{2\eta+1}{(1+\eta)^2} \left(f_V^0 - f_V^1 \frac{A-2Z}{A} \right)^2 I_1(u_0) \right\} + [f_A^0 \Omega_0(0)]^2 I_{00}(u_0) + 2 f_A^0 f_A^1 \Omega_0(0) \Omega_1(0) I_{01}(u_0) \right. \\ \left. + [f_A^1 \Omega_1(0)]^2 I_{11}(u_0) \right). \quad (15)$$

The quantities I_{ρ} entering Eq. (13) are defined as

$$I_{\rho}(u_0) = (1+\rho) u_0^{-(1+\rho)} \int_0^{u_0} x^{1+\rho} |F(x)|^2 dx, \quad \rho = 0, 1, \quad (16)$$

where $F(u_0 \xi^2)$ the nuclear form factor and

$$u_0 = q^2 b^2 / 2 \quad (17)$$

with b being the harmonic oscillator size parameter. The integrals $I_{\rho\rho'}$, with $\rho, \rho' = 0, 1$, result by following the standard procedure of the multipole expansion of the $e^{-i\mathbf{q}\cdot\mathbf{r}}$ in Eq. (9). One finds

$$I_{\rho\rho'}(u_0) = 2 \int_0^1 \xi d\xi \sum_{\lambda, \kappa} \frac{\Omega_{\rho}^{(\lambda, \kappa)}(u_0 \xi^2)}{\Omega_{\rho}(0)} \frac{\Omega_{\rho'}^{(\lambda, \kappa)}(u_0 \xi^2)}{\Omega_{\rho'}(0)}, \quad \rho, \rho' = 0, 1. \quad (18)$$

For the evaluation of the differential rate, which is the main subject of the present work, it will be more convenient to use the variables (v, u) instead of the variables (v, ξ) . Thus we get

$$d\sigma(u, v) = \sigma_0 \left(\frac{m_x}{m_N} \right)^2 \frac{1}{(1+\eta)^2} \left(A^2 \left\{ \left[\left(\frac{v}{c} \right)^2 \left(f_V^0 - f_V^1 \frac{A-2Z}{A} \right)^2 + \left(f_S^0 - f_S^1 \frac{A-2Z}{A} \right)^2 \right] F^2(u) \right. \right. \\ \left. \left. - \frac{1}{(2\mu_r b)^2} \frac{2\eta+1}{(1+\eta)^2} \left(f_V^0 - f_V^1 \frac{A-2Z}{A} \right)^2 u F^2(u) \right\} + [f_A^0 \Omega_0(0)]^2 F_{00}(u) + 2 f_A^0 f_A^1 \Omega_0(0) \Omega_1(0) F_{01}(u) \right. \\ \left. + [f_A^1 \Omega_1(0)]^2 F_{11}(u) \right) \frac{du}{2(\mu_r b v)^2} \quad (19)$$

$$u = q^2 b^2 / 2, \quad \mu_r = \frac{m_x}{1+\eta} \quad (20)$$

where μ_r is the reduced mass and the quantity u is related to the experimentally measurable energy transfer Q via the relations

$$Q = Q_0 u, \quad Q_0 = \frac{1}{Am_N b^2}. \quad (21)$$

Let us now assume that the LSP is moving with velocity v_z with respect to the detecting apparatus. Then, the detection rate for a target with mass m is given by

$$R = \frac{dN}{dt} = \frac{\rho(0)}{m_\chi} \frac{m}{Am_N} |v_z| \sigma(u, v) \quad (22)$$

where $\rho(0) = 0.3 \text{ GeV/cm}^3$ is the LSP density in our vicinity. This density has to be consistent with the LSP velocity distribution (see next section).

The differential rate can be written as

$$dR = \frac{\rho(0)}{m_\chi} \frac{m}{Am_N} |v_z| d\sigma(u, v) \quad (23)$$

where $d\sigma(u, v)$ is given by Eq. (19)

III. CONVOLUTION OF THE EVENT RATE

We have seen that the event rate for LSP-nucleus scattering depends on the relative LSP-target velocity. In this section we will examine the consequences of Earth's revolution around the Sun (the effect of its rotation around its axis will be negligible), i.e. the modulation effect. This can be accomplished by convoluting the rate with the velocity distribution. Such a consistent choice can be a Maxwell distribution [1]

$$f(v') = (\sqrt{\pi} v_0)^{-3} e^{-(v'/v_0)^2} \quad (24)$$

provided that

$$v_0 = \sqrt{(2/3)\langle v^2 \rangle} = 220 \text{ km/s}. \quad (25)$$

For our purposes it is convenient to express the above distribution in the laboratory frame, i.e.

$$f(\mathbf{v}, \mathbf{v}_E) = (\sqrt{\pi} v_0)^{-3} e^{-(\mathbf{v} + \mathbf{v}_E)^2 / v_0^2} \quad (26)$$

where \mathbf{v}_E is the velocity of Earth with respect to the center of the distribution. Choosing a coordinate system in which $\hat{\mathbf{x}}_2$ is the axis of the galaxy, $\hat{\mathbf{x}}_3$ is along the Sun's direction of motion (\mathbf{v}_0) and $\hat{\mathbf{x}}_1 = \hat{\mathbf{x}}_2 \times \hat{\mathbf{x}}_3$, we find that the position of the axis of the ecliptic is determined by the angle $\gamma \approx 29.80$ (galactic latitude) and the azimuthal angle $\omega = 186.3^\circ$ measured on the galactic plane from the $\hat{\mathbf{x}}_3$ axis [5].

Thus, the axis of the ecliptic lies very close to the $x_2 x_3$ plane and the velocity of Earth is

$$\mathbf{v}_E = \mathbf{v}_0 + \mathbf{v}_1 = \mathbf{v}_0 + v_1 (\sin \alpha \hat{\mathbf{x}}_1 - \cos \alpha \cos \gamma \hat{\mathbf{x}}_2 + \cos \alpha \sin \gamma \hat{\mathbf{x}}_3). \quad (27)$$

Furthermore

$$\mathbf{v}_0 \cdot \mathbf{v}_1 = v_0 v_1 \frac{\cos \alpha}{\sqrt{1 + \cot^2 \gamma \cos^2 \omega}} \approx v_0 v_1 \sin \gamma \cos \alpha \quad (28)$$

where v_0 is the velocity of the Sun around the center of the galaxy, v_1 is the speed of Earth's revolution around the Sun, α is the phase of Earth's orbital motion and $\alpha = 2\pi(t - t_1)/T_E$, where t_1 is around second of June and $T_E = 1 \text{ yr}$.

The mean value of the differential event rate of Eq. (23) is defined by

$$\left\langle \frac{dR}{du} \right\rangle = \frac{\rho(0)}{m_\chi} \frac{m}{Am_N} \int f(\mathbf{v}, \mathbf{v}_E) |v_z| \frac{d\sigma(u, v)}{du} d^3 \mathbf{v}. \quad (29)$$

It can be more conveniently expressed as

$$\left\langle \frac{dR}{du} \right\rangle = \frac{\rho(0)}{m_\chi} \frac{m}{Am_N} \sqrt{\langle v^2 \rangle} \left\langle \frac{d\Sigma}{du} \right\rangle \quad (30)$$

where

$$\left\langle \frac{d\Sigma}{du} \right\rangle = \int \frac{|v_z|}{\sqrt{\langle v^2 \rangle}} f(\mathbf{v}, \mathbf{v}_E) \frac{d\sigma(u, v)}{du} d^3 \mathbf{v}. \quad (31)$$

Thus, taking the polar axis in the direction \mathbf{v}_E , we get

$$\begin{aligned} \left\langle \frac{d\Sigma}{du} \right\rangle &= \frac{4}{\sqrt{6} \pi v_0^4} \int_{v_s}^{\infty} v^3 dv \\ &\times \int_{-1}^1 |\xi| d\xi e^{-(v^2 + v_E^2 + 2vv_E\xi)/v_0^2} \frac{d\sigma(u, v)}{du} \end{aligned} \quad (32)$$

or

$$\left\langle \frac{d\Sigma}{du} \right\rangle = \frac{2}{\sqrt{6} \pi v_E^2} \int_{v_s}^{\infty} v dv F_0 \left(\frac{2vv_E}{v_0^2} \right) e^{-(v^2 + v_E^2)/v_0^2} \frac{d\sigma(u, v)}{du} \quad (33)$$

with

$$v_s = v_0 a \sqrt{u} \quad (34)$$

$$a = \frac{1}{\sqrt{2} \mu_r b v_0} \quad (35)$$

and

$$F_0(\chi) = \chi \sinh \chi - \cosh \chi + 1. \quad (36)$$

Introducing the parameter

$$\delta = \frac{2v_1}{v_0} = 0.27, \quad (37)$$

expanding in powers of δ and keeping terms up to linear in it we can write Eq. (33) as

$$\begin{aligned}
 \left\langle \frac{d\Sigma}{du} \right\rangle = & \sigma_0 \left(\frac{m_x}{m_N} \right)^2 \frac{1}{(1+\eta)^2} \left(A^2 \left[\beta_0^2 \left(f_V^0 - f_V^1 \frac{A-2Z}{A} \right)^2 \bar{F}_1(u) + \left(f_S^0 - f_S^1 \frac{A-2Z}{A} \right)^2 \bar{F}_0(u) \right. \right. \\
 & - \left. \frac{1}{(2\mu_r b)^2} \frac{2\eta+1}{(1+\eta)^2} \left(f_V^0 - f_V^1 \frac{A-2Z}{A} \right)^2 u \bar{F}_0(u) \right] + [f_A^0 \Omega_0(0)]^2 \bar{F}_{00}(u) + 2 f_A^0 f_A^1 \Omega_0(0) \Omega_1(0) \bar{F}_{01}(u) \\
 & \left. + [f_A^1 \Omega_1(0)]^2 \bar{F}_{11}(u) \right) (a^2/e) \tag{38}
 \end{aligned}$$

with $\beta_0 = v_0/c$. The quantities $\bar{F}_0, \bar{F}_1, \bar{F}_{00}, \bar{F}_{01}, \bar{F}_{11}$ are obtained from the corresponding form factors via the equations

$$\bar{F}_0(u) = F^2(u) [\Phi_0^{(0)}(a\sqrt{u}) + 0.135 \cos \alpha \Phi_0^{(1)}(a\sqrt{u})] \tag{39}$$

$$\bar{F}_{\rho, \rho'}(u) = F_{\rho, \rho'}(u) [\Phi_0^{(0)}(a\sqrt{u}) + 0.135 \cos \alpha \Phi_0^{(1)}(a\sqrt{u})] \tag{40}$$

$$\bar{F}_1(u) = F^2(u) [\Phi_1^{(0)}(a\sqrt{u}) + 0.135 \cos \alpha \Phi_1^{(1)}(a\sqrt{u})] \tag{41}$$

$$\Phi_k^{(l)}(x) = \frac{2}{\sqrt{6\pi}} \int_x^\infty dy y^{2k-1} [\exp(-y^2)] F_l(2y) \tag{42}$$

with $F_0(\chi)$ given in Eq. (34) and

$$F_1(\chi) = 2 \left[\left(\frac{\chi^2}{4} + 1 \right) \cosh \chi - \chi \sinh \chi - 1 \right]. \tag{43}$$

For the cases we considered in this work we find that the quantities $\bar{F}_{\rho, \rho'}(u)$ are almost the same for all isospin channels. We believe this to be a more general result. The value of 0.135 was obtained using $\sin \gamma \approx 0.5$

Combining Eqs. (30), (37) and (39)–(42) we obtain

$$\left\langle \frac{dR}{du} \right\rangle = \bar{R} t^0 R0 [1 + H(u) \cos \alpha]. \tag{44}$$

In the above expressions \bar{R} is the rate obtained in the conventional approach [4] by neglecting the momentum transfer dependence of the differential cross section, i.e. by integrating Eq. (30) after the form factors \bar{F} entering Eq. (37) have been neglected. The parameter t^0 is the additional factor needed when the form factors are included and the total event rate is convoluted with the velocity distribution. $R0$ is the relative differential rate, i.e. the differential rate divided by the total rate, in the absence of modulation, i.e.

$$R0 = \frac{1}{t^0} \frac{dr^{(0)}}{du}. \tag{45}$$

Note that in the above expressions t^0 was defined so that the quantity $R0$ is normalized to unity when integrated from u_{min} to infinity. From Eqs. (39)–(42) we see that if we consider each mode separately the differential modulation amplitude H takes the form

$$H(u) = 0.135 \frac{\Phi_k^{(0)}(a\sqrt{u})}{\Phi_k^{(1)}(a\sqrt{u})}. \tag{46}$$

Thus in this case H depends only on $a\sqrt{u}$ which coincides with the parameter x of Ref. [12]. This means that, if we neglect the coherent vector contribution, which, as we have mentioned, is justified, H essentially depends only on the momentum transfer, the reduced mass and the size of the nucleus.

Integrating Eq. (44) we get

$$R = \bar{R} t^0 [1 + h(u_0, Q_{min}) \cos \alpha] \tag{47}$$

where Q_{min} is the energy transfer cutoff imposed by the detector. The effect of folding with LSP velocity on the total rate is taken into account via the quantity t^0 . All other SUSY parameters have been absorbed in \bar{R} . Strictly speaking the quantity h also depends on the SUSY parameters. It does not depend on them, however, if one considers the scalar, spin, etc., modes separately.

Returning to the differential rate it is sometimes convenient, as we will see later, to write it in a slightly different form

$$\left\langle \frac{dR}{du} \right\rangle = \bar{R} t^0 (R0 + R1 \cos \alpha). \tag{48}$$

$R1$ contains the effect of modulation and is given by

$$R1 = \frac{1}{t^0} \frac{dr^{(1)}}{du}. \tag{49}$$

The meaning of $R0$ and $R1$ will become more transparent if we consider each mode separately. Thus for the scalar interaction we get $\bar{R} \rightarrow \bar{R}_{scalar}$ and

$$\frac{dr^{(0)}}{du} = a^2 F^2(u) \Phi_0^{(0)}(a\sqrt{u}) \tag{50}$$

$$\frac{dr^{(1)}}{du} = 0.135 a^2 F^2(u) \Phi_0^{(1)}(a\sqrt{u}). \tag{51}$$

For the spin interaction we get a similar expression except that $\bar{R} \rightarrow \bar{R}_{spin}$ and $F^2 \rightarrow F_{\rho, \rho'}$. Finally for completeness we will consider the less important vector contribution. We get $\bar{R} \rightarrow \bar{R}_{vector}$ and

TABLE Ia. The quantity t^0 for the target ${}_{82}\text{Pb}^{207}$. t^0 takes into account the velocity dependence of the event rate and the folding with the LSP velocity distribution. It is computed for various LSP masses in the allowed SUSY parameter space. The scalar, the vector coherent ($k=1$) and the spin contributions are included. In the latter (11), (01) and (11) indicate the possible isospin channels.

Mode	Q_{min} (keV)	LSP mass in GeV						
		30	50	80	100	125	250	500
Scalar	0	1.23	0.728	0.413	0.316	0.246	0.123	0.0761
	20	0.404	0.331	0.209	0.164	0.129	0.0668	0.0468
	40	0	2×10^{-4}	5×10^{-4}	7×10^{-4}	6×10^{-4}	5×10^{-4}	4×10^{-4}
Vector	0	3.349	1.735	0.902	0.671	0.509	0.248	0.151
Spin (11)	0	1.57	1.298	0.949	0.793	0.661	0.394	0.266
Spin (11)	20	0.082	0.512	0.367	0.344	0.312	0.216	0.155
Spin (00)	0	1.45	1.13	0.793	0.655	0.542	0.318	0.213
Spin (01)	0	1.51	1.21	0.866	0.719	0.597	0.353	0.237

$$\frac{dr^{(0)}}{du} = a^2 F^2(u) \left[\Phi_1^{(0)}(a\sqrt{u}) - \frac{1}{(2\mu_r b)^2} \frac{2\eta+1}{(1+\eta)^2} u \Phi_0^{(0)}(a\sqrt{u}) \right] \quad (52)$$

$$\frac{dr^{(1)}}{du} = 0.135 a^2 F^2(u) \times \left[\Phi_1^{(1)}(a\sqrt{u}) - \frac{1}{(2\mu_r b)^2} \frac{2\eta+1}{(1+\eta)^2} u \Phi_0^{(1)}(a\sqrt{u}) \right]. \quad (53)$$

We see that, if we consider each mode separately, $R0$ and $R1$ are independent of all the supersymmetry (SUSY) parameters except for m_χ . They depend upon the nuclear physics via the relevant form factors.

IV. RESULTS AND DISCUSSION

The three basic ingredients of the LSP-nucleus scattering are the input SUSY parameters, a quark model for the nucleon and the structure of the nuclei involved. The latter enters through the nuclear form factor and the spin response function [5]. Experimentally one is interested in the differ-

ential rate. In the present work we found it convenient to express it in the manner given by Eq. (44), i.e. in terms of the parameters $\bar{R}, t^0, R0$ and the convolution amplitude H . The parameter \bar{R} contains all the information regarding the SUSY model. It has been discussed previously (see e.g. Refs. [4,5]) and it is not the subject of the present work. The other parameters will be discussed below. One is also interested in the total rate [see Eq. (47)]. For this, instead of $R0$ and H , one needs the modulation amplitude h .

The parameter t^0 expresses the modification of the event rate due to the dependence of the cross-section on the velocity of the LSP and the folding with the LSP velocity distribution. The obtained results, which depend on the LSP mass, the nuclear form factors and the detector energy cutoff, Q_{min} , are presented in Tables Ia and IIa for four nuclear targets of experimental interest. For comparison the same results, but without the nuclear form factors, are presented in Table IIIa for one medium and one heavy target (the form factor effect is not expected to be significant for light nuclei [5]). We see from these tables that t^0 changes appreciably, once the form factor effects are included, both for a large LSP mass and large energy cutoff Q_{min} .

The obtained results for h , the modulation of the total event rate, are shown in Table Ib for Pb and in Table IIb for some other nuclei of experimental interest. The results with-

TABLE Ib. The same as in Table I(a) for the modulation amplitude h .

Mode	Q_{min} (keV)	LSP mass in GeV						
		30	50	80	100	125	250	500
Scalar	0	0.0295	0.0151	0.0054	0.0022	-0.0001	-0.0005	-0.0059
	20	0.1543	0.0774	0.0401	0.0292	0.0211	0.0070	0.0013
	40	0.2525	0.1598	0.0991	0.0784	0.0620	0.0314	0.0177
Vector	0	0.0543	0.0621	0.0571	0.0560	0.0553	0.0545	0.0543
Spin (11)	0	0.0460	0.0307	0.9266	0.0219	0.0184	0.0113	0.0066
Spin (11)	20	0.1659	0.0926	0.0549	0.0444	0.0371	0.0234	0.0151
Spin (00)	0	0.0421	0.0349	0.0238	0.0195	0.0163	0.0100	0.0056
Spin (01)	0	0.0440	0.0369	0.0252	0.0207	0.0174	0.0107	0.0061

TABLE IIa. The quantity t^0 for the experimentally interesting targets $_{53}\text{I}^{127}$, $_{11}\text{Na}^{23}$ and $_{13}\text{Al}^{27}$ (for definitions see Table Ia).

Target	Q_{min} (keV)	LSP mass in GeV							
		10	20	30	50	80	100	125	250
I	0	2.16		1.50	1.04	0.689	0.566	0.469	0.287
	20	0.0		0.089	0.170	0.162	0.144	0.127	0.0855
	45	0.0		0.0014	0.0124	0.0198	0.0201	0.0193	0.0150
Spin (11)	0	2.13		1.40	0.960	0.651	0.553	0.473	0.323
	20	0.0		0.075	0.153	0.167	0.164	0.158	0.137
	45	0.0		0.0018	0.0288	0.0483	0.0587	0.0674	0.0781
Na	0	2.33	2.32	2.31	2.30	2.30	2.30	2.30	2.30
	8	0.454	1.19	1.49	1.69	1.69	1.69	1.69	1.69
	16	0.064	0.570	0.907	1.19	1.19	1.19	1.19	1.19
Al	0	2.32	2.31	2.30	2.29	2.29	2.29	2.29	2.29
	0.5	2.11	2.22	2.24	2.25	2.25	2.25	2.25	2.25

out the nuclear form factor are shown in Table IIIb. From these tables we notice that for the Pb target the nuclear form factor suppresses the modulation amplitude for heavy LSP's for all values of Q_{min} . It is however more pronounced in the case $Q_{min}=0$, since in this case, in the presence of the nuclear form factor, the small energy transfer components cancel almost completely the contribution of the large energy transfer. For the intermediate target, *I*, the trends are similar but less pronounced.

From the Tables I(b) and II(b) we see that typically h is quite small, $\leq 5\%$. In view of Ref. [12], however, it is not very surprising that it can become much larger for a fairly light LSP and large detector energy cutoff. In other words in such cases, as the cutoff energy increases, the modulated amplitude decreases less than the unmodulated one. There seems, therefore, to be a kind of trade-off between the total rate and the modulation amplitude. Thus the detector imposed cutoffs may yield the bonus of a sizable modulation effect. Note, however, that in such circumstances, especially due to form factor effects, the total event rate is suppressed and it may not be detectable.

The quantity which the experiments attempt to measure is the differential rate. In the present work we found it convenient to work with the relative differential event rate with respect to the energy transfer Q , i.e. the differential rate divided by the total rate. Instead of Q we found it convenient to express our results in terms of the dimensionless parameter u introduced above [see Eq. (20)]. The parameter u is related to the energy transfer by $Q=Q_0u$ with Q_0 given by Eq. (21).

We focused our attention on the modulation amplitude which is described either by the parameter H [see Eq. (46)] or by $R1$ [see Eq. (49)]. $R1$ and H are independent of the SUSY parameters and the structure of the nucleon. $R1$ mildly depends on the nuclear structure; i.e., it depends on the reduced mass of the system, the nuclear form factor and the lower energy cutoff imposed by the detectors. H is even independent of the nuclear form factor, but in addition to the energy transfer, it depends on the mass of the nucleus and the LSP mass.

Summarizing our results we can say the following:

- (1) *The nucleus $_{82}\text{Pb}^{207}$* [4,5]. In this case $Q_0=40$ keV.

TABLE IIb. The same as in Table IIa for the modulation amplitude h .

Target	Q_{min} (keV)	LSP mass in GeV							
		10	20	30	50	80	100	125	250
I	0	0.0508		.0361	0.0241	0.0139	0.0102	0.0072	0.0013
	20	0.0		0.1298	0.0734	0.0426	0.0331	0.0258	0.0126
	45	0.0		0.2194	0.1294	0.0740	0.0588	0.0474	0.0267
Spin (11)	0	0.0501		0.0344	0.0241	0.0180	0.0166	0.0157	0.0149
	20	0.0		0.1309	0.0793	0.0568	0.0512	0.0471	0.0400
	45	0.0		0.2215	0.1402	0.1018	0.0910	0.0809	0.0630
Na	0	0.0540	0.0539	0.0537	0.0535	0.0535	0.0535	0.0535	0.0535
	8	0.1334	0.0906	0.0793	0.0715	0.0715	0.0715	0.0715	0.0715
	16	0.2039	0.1237	0.1030	0.0911	0.0911	0.0911	0.0911	0.0911
Al	0	0.0538	0.0538	0.0596	0.0534	0.0534	0.0534	0.0534	0.0534
	0.5	0.0598	0.0563	0.0553	0.0545	0.0545	0.0545	0.0545	0.0545

TABLE IIIa. The quantity t^0 for the targets $_{82}\text{Pb}^{207}$ and $_{53}\text{I}^{127}$ neglecting the influence of the nuclear form factor (for definitions see Table I).

Target	Q_{min} (keV)	LSP mass in GeV						
		30	50	80	100	125	250	500
Pb	0	2.330	2.331	2.331	2.329	2.322	2.139	1.788
Scalar	20	0.1645	0.8180	1.421	1.624	1.773	1.839	1.613
	40	0.0077	0.2525	0.8320	1.107	1.334	1.606	1.449
I	0	2.331	2.331	2.331	2.331	2.322	2.322	2.320
Scalar	20	0.3676	1.040	1.528	1.685	1.805	2.010	2.008
	45	0.0253	0.3380	0.8631	1.087	1.287	1.666	1.660

We considered both the coherent and spin contributions for

$$m_\chi = 30, 50, 80, 100, 125, 250, 500 \text{ GeV and}$$

$$Q_{min} = 0, 20, 40 \text{ keV}$$

employing the harmonic oscillator form factors of Ref. [22]. Our results are presented in Figs. 1(a)–1(j). For comparison we present in Figs. 2(a)–2(f) results obtained by disregarding the form factor dependence of the cross-section. In this special case the variable x of Ref. [12] is more appropriate, but we decided to use u to make the comparison with the exact results easier. Since, as we have mentioned, the parameter H is independent of the form factor, it is not shown in Fig. 2. It is also independent of Q_{min} and thus it is shown only for $Q_{min} = 0$.

It is known [5] that the form factor dependence is more dramatic for a large reduced mass, i.e. a heavy nucleus like Pb and massive LSP's. The curves of Fig. 1 and Fig. 2 look similar, but note the range of u . The effect of the form factor is to make the differential rate drop much faster as a function of u , i.e. the energy transfer. The effect of the form factor is a bit less dramatic in the case of the spin induced rate. We see that H rises with u and for the same u it decreases with the LSP mass. It can become as large as 10% for a light LSP [see Fig. 1(c)]. The maximum to minimum ratio can be as high as 1.2. Furthermore, we notice that the event rate drops sharply after $u = 0.4$, i.e. $Q = 16$ keV. Thus, the most favored region is around $u = 0.2$ or $Q = 8$ keV [see Fig. 1(b)]. We also see that H is negative at small u and becomes positive as u increases. Notice, however, that the event rate is large at low u [see Fig. 1(a)]. Hence we have cancellations in the

total modulation amplitude. The analogous results for $Q_{min} = 20$ keV are shown in Figs. 1(d)–1(e). The latter results are shifted compared to the previous ones by $\Delta u = 0.125$ but they appear otherwise similar. This similarity is misleading, since it is the result of the normalization adopted [the area under each of the curves $R0$ vs u , Figs. 1(a), 1(d), 1(f) and 1(h), is unity]. Notice furthermore that the absolute rates are down about a factor of 3 from those at $Q_{min} = 0$. We see from Table I(a) that the total event rates are very much suppressed for $Q_{min} = 40$ keV. Thus if such cutoffs are required by the detector, the process is unobservable. We also present results for the spin contribution for the isospin (11) channel in Figs. 1(f)–1(g) for $Q_{min} = 0$. Our results for $Q_{min} = 20$ keV compared to those of $Q_{min} = 0$ show a similar trend as those of Figs. 1(d) and 1(e) when compared to those of Figs. 1(a) and 1(b). The other isospin channels show behavior similar to the (11) channel [5]. Thus we can say in general that the differential rate due to the spin contribution falls quite a bit slower compared to the coherent rate as a function of u . We also know that the total rate shows a similar trend with respect to u_0 [5]. Furthermore, the quantity $R1$ is a bit broader, which means that the modulation effect is somewhat favored in the spin contribution since a broader energy window around the maximum can be selected. For purposes of comparison, we present in Figs. 1(h)–1(j) the analogous results for $Q_{min} = 0$ obtained for the less important coherent vector contribution. We see that, in addition to the couplings, the LSP velocity distribution favors the vector contribution (H now can be as large as 0.15). This, of course, may not be enough to overcome the suppression factor β_0^2 [see Eq. (36)] due to the Majorana nature of the LSP.

TABLE IIIb. The same as in Table IIIa for the modulation amplitude h .

Target	Q_{min} (keV)	LSP mass in GeV						
		30	50	80	100	125	250	500
Pb	0	0.0542	0.0542	0.0541	0.0541	0.0534	0.04412	0.0320
Scalar	20	0.1713	0.1089	0.0823	0.0749	0.0691	0.0523	0.0362
	40	0.2620	0.1561	0.1089	0.0946	0.0841	0.0581	0.0401
I	0	0.0541	0.0542	0.0542	0.00542	0.0542	0.00534	0.0530
Scalar	20	0.1421	0.0980	0.0785	0.0732	0.0694	0.0621	0.0620
	45	0.2296	0.1453	0.1065	0.0961	0.0874	0.0726	0.0720

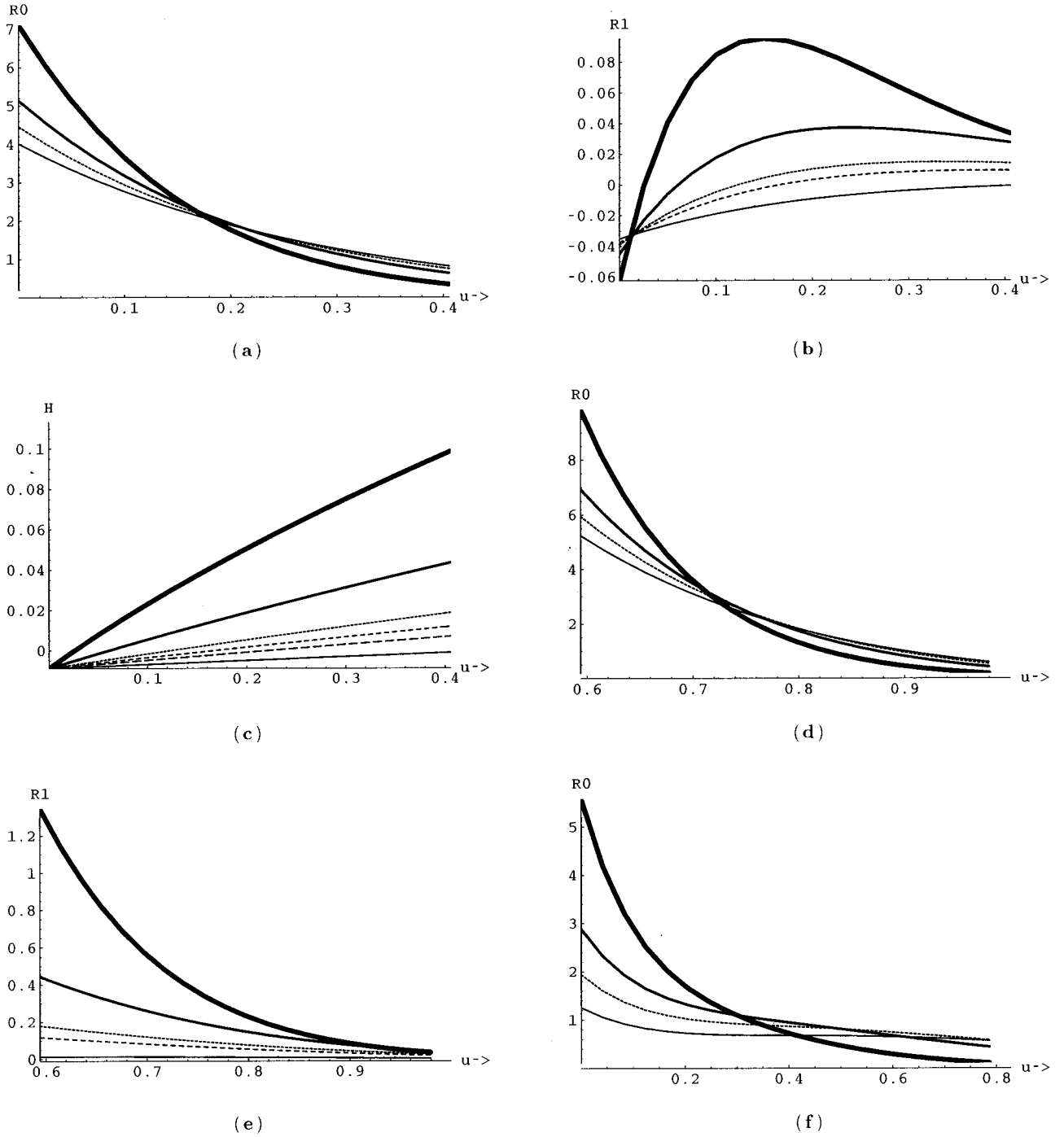


FIG. 1. The relative differential event rate $R0$ and the amplitudes for modulation $R1$ and H vs u for the target ${}_{82}\text{Pb}^{207}$ (for the definitions see text). In the case of the modulated amplitudes the effect of the phase of Earth (the factor $\cos \alpha$) has not been included in the plots. The curves shown correspond to LSP masses as follows: (i) Thick solid line $\Leftrightarrow m_\chi = 30$ GeV. (ii) Solid line $\Leftrightarrow m_\chi = 50$ GeV. (iii) Dotted line $\Leftrightarrow m_\chi = 80$ GeV. (iv) Dashed line $\Leftrightarrow m_\chi = 100$ GeV. (v) Intermediate dashed line $\Leftrightarrow m_\chi = 125$ GeV. (vi) Fine solid line $\Leftrightarrow m_\chi = 250$ GeV. (vii) Long dashed line $\Leftrightarrow m_\chi = 500$ GeV. If some curves of the above list seem to have been omitted, it is understood that they fall on top of (vi). Note that, due to our normalization of $R0$, the area under the corresponding curve is unity. (a) $R0$ for the scalar contribution and $Q_{min} = 0$. (b) The amplitude $R1$ for the scalar contribution and $Q_{min} = 0$. (c) The modulation amplitude H , i.e. the ratio of $R1$ divided by $R0$ for $Q_{min} = 0$. (d) The same as in (a) for $Q_{min} = 20$ keV. (e) The same as in (b) for $Q_{min} = 20$ keV. (f) The same as in (a) for the spin contribution in the isospin (11) channel. For the other isospin channels the results are similar. (g) The same as in (b) for the spin contribution in the (11) channel. (h) The same as in (a) for the vector coherent contribution. (i) The same as in (b) for the vector coherent contribution. (j) The same as in (c) for the vector coherent contribution.

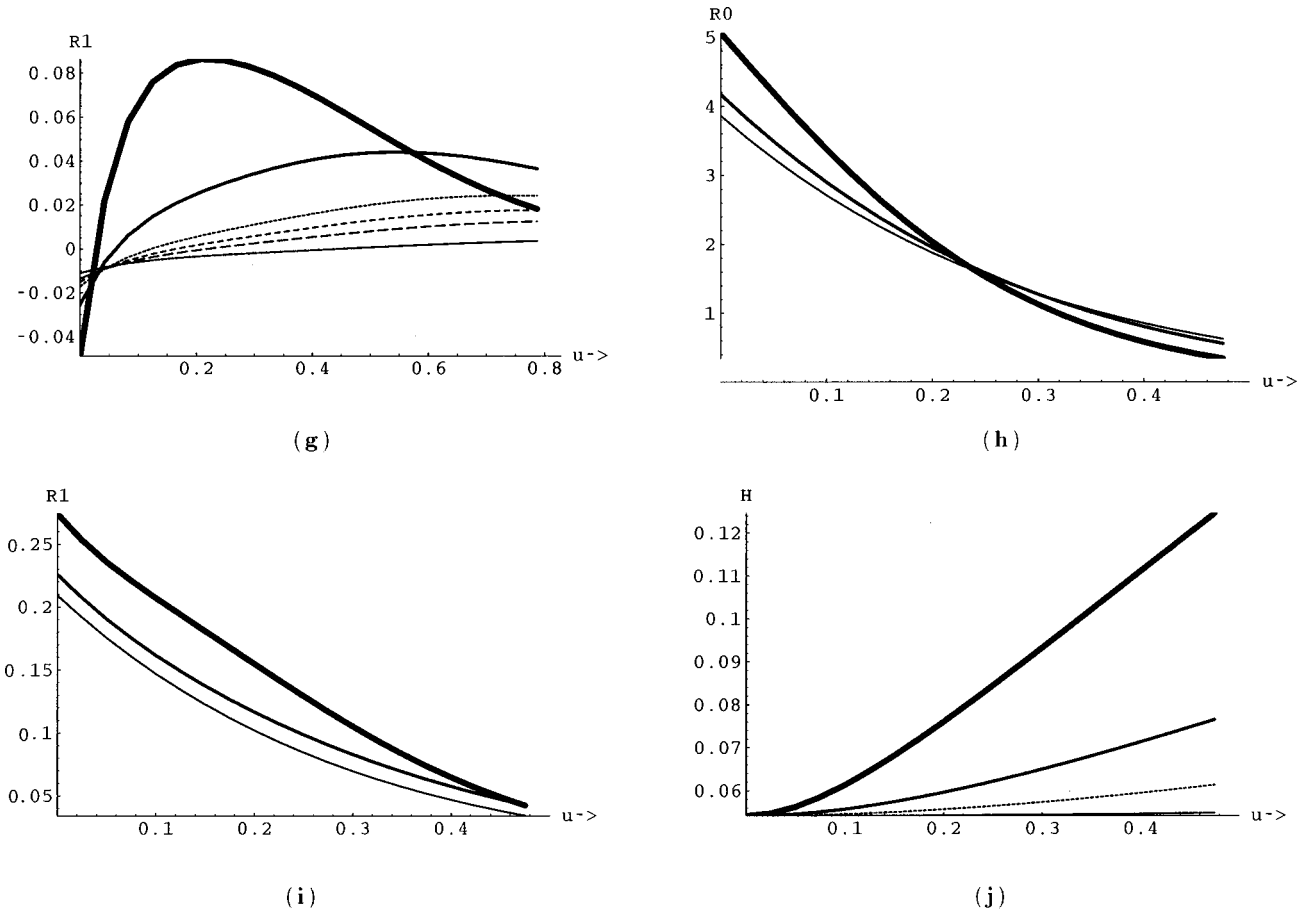


FIG. 1. (Continued).

(2) *The nucleus ${}_{53}\text{I}^{127}$.* This nucleus is of great experimental interest [21] due to the advantages of the NaI detector. In this case $Q_0 = 60$ keV. We show results for the coherent scalar interaction employing the harmonic oscillator form factors of Ref. [22] for

$$m_\chi = 30, 50, 80, 100, 125, 250 \text{ GeV} \text{ and } Q_{\min} = 0.45 \text{ keV}.$$

Even though for $Q_{\min} = 45$ keV, the total rate is suppressed (see Table IIa), and for the benefit of the experimentalists we will present the corresponding results for the differential rate. We do not show the differential rate for $m_\chi = 10$ since it falls off too fast as a function of u . So there is no advantage in going to an energy window. Our results are shown in Figs. 3(a)–3(c) and Figs. 3(d) and 3(e) for $Q_{\min} = 0$ and 45 keV respectively. H now can be as large as 0.25. Results for $Q_{\min} = 0$ keV are also shown in Figs. 3(g) and 3(h) in the case of the spin contribution for the isospin (11) channel. The other channels show a similar behavior. The spin form factors were taken from Ref. [7]. The form factor dependence of the differential rate cannot be ignored, but it is less dramatic than that occurring in the case of the heavier nucleus ${}_{82}\text{Pb}^{207}$ and it is not shown.

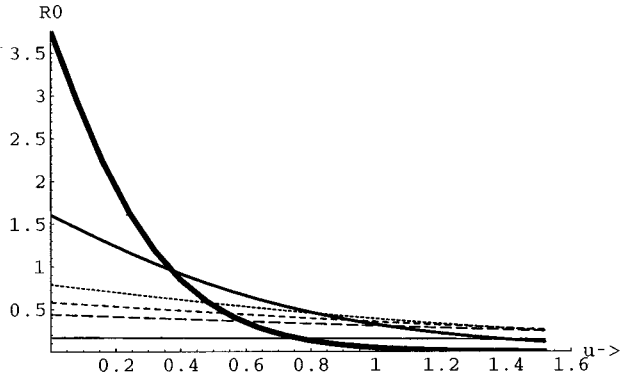
(3) *The nucleus ${}_{11}\text{Na}^{23}$.* This nucleus is a part of the same detector as in the previous one. Here $Q_0 = 630$ keV. Even though for this light nucleus the spin contribution may be relatively more important compared to the coherent one, we

only considered in this work the coherent contribution in a fashion analogous to the Al case discussed below. The parameters t^0 and h are shown in Tables II(a) and II(b) respectively. In this case the detector energy cutoff is 8–16 keV. Our results for the differential rate for a zero energy cutoff are similar to those for Al listed below. For $Q_{\min} = 16$ keV they are shown in Figs. 4(a) and 4(b). We see that in all cases the differential rate falls off real fast as a function of u . This is not surprising since for such a light system the momentum transferred to the nucleus cannot be large.

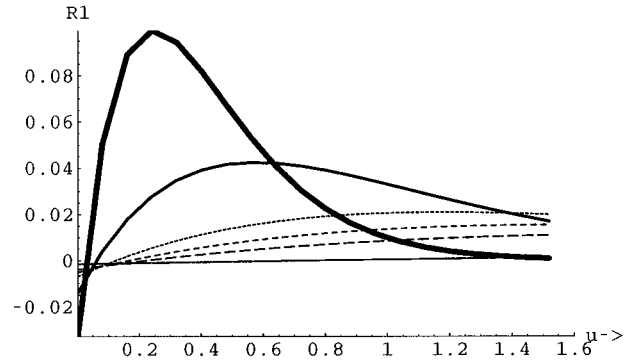
(4) *The nucleus ${}_{13}\text{Al}^{27}$.* A detector with this nucleus has the advantage of very low energy threshold $Q_{\min} = 0.5$ keV. In this case $Q_0 = 480$ keV. Again only the coherent scalar contribution was considered. Both harmonic oscillator and Woods-Saxon form factors were tried. The difference between them was small. The results presented were obtained with the Woods-Saxon form factors with $c = 3.07$ and $a_0 = 0.519$ fm [23]. The parameters t^0 and h for various LSP masses and cutoffs are given in Tables II(a) and II(b) respectively. In our plots we considered the values of $m_\chi = 10, 20, 30, 50$ GeV. For larger masses the results remain unchanged. For $Q_{\min} = 0.5$ keV our results for the differential rate are shown in Figs. 5(a)–5(c).

V. CONCLUSIONS

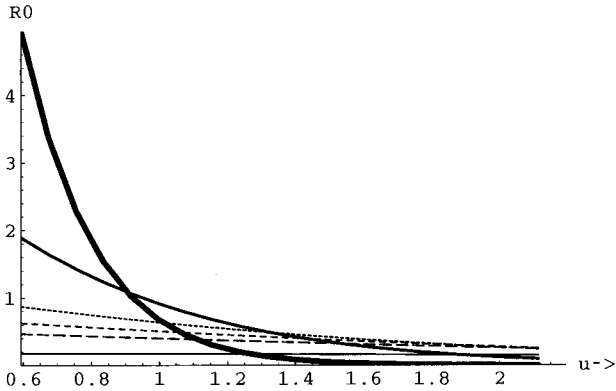
Detectable rates for the LSP-nucleus scattering for some choices in the allowed SUSY parameter space are possible



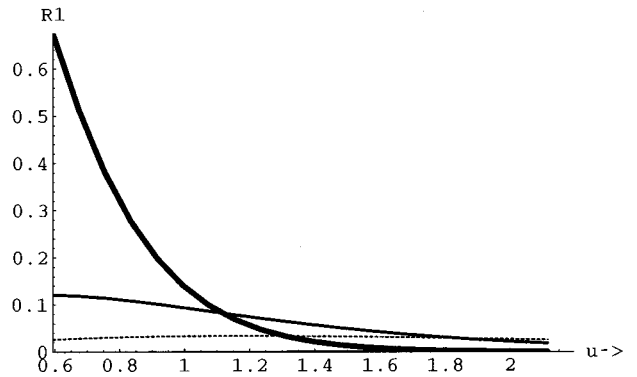
(a)



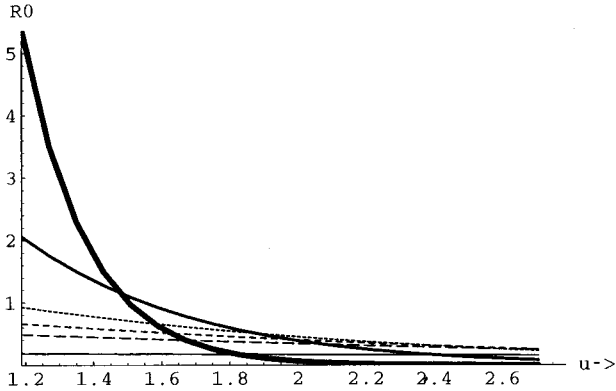
(b)



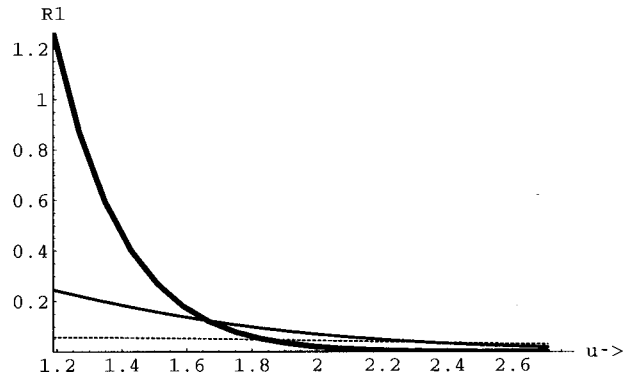
(c)



(d)



(e)



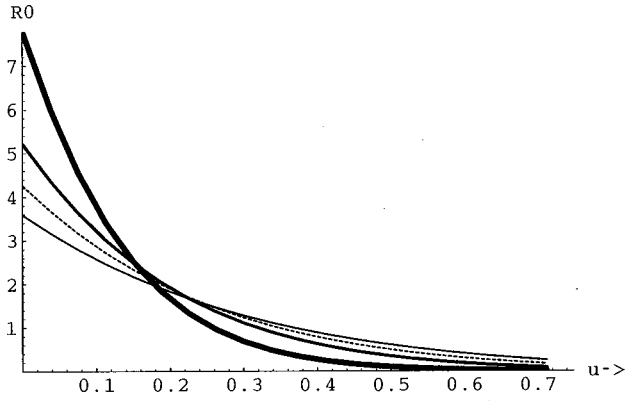
(f)

FIG. 2. The same as in Fig. 1 for the coherent mode, but here we have disregarded the form factor dependence of the LSP-nucleus cross-section. H is the same as in the previous figure and it is not shown. (a) $R0$ for $Q_{min}=0$. (b) $R1$ for $Q_{min}=0$. (c) The same as (a) for $Q_{min}=20$ keV. (d) The same as (b) for $Q_{min}=20$ keV. (e) The same as (a) for $Q_{min}=45$ keV. (f) The same as (b) for $Q_{min}=45$ keV. The style of the curves is the same as in Fig. 1.

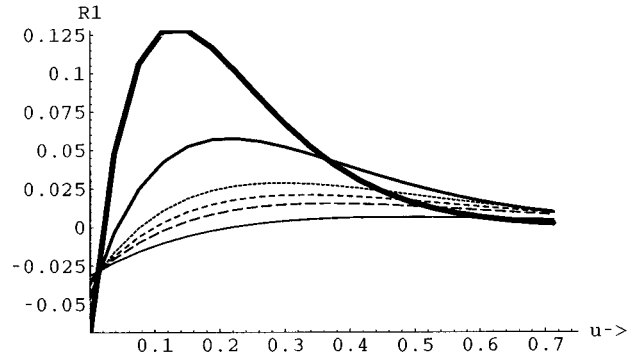
[5]. Similar results have been obtained in the form of scatterplots by Nath and Arnowitt [18], Bottino *et al.* [16] and more will appear elsewhere [20]. Since, anyway, the event rate is indeed very low, one should try to exploit the modulation

effect, i.e. the dependence of the event rate on the motion of Earth.

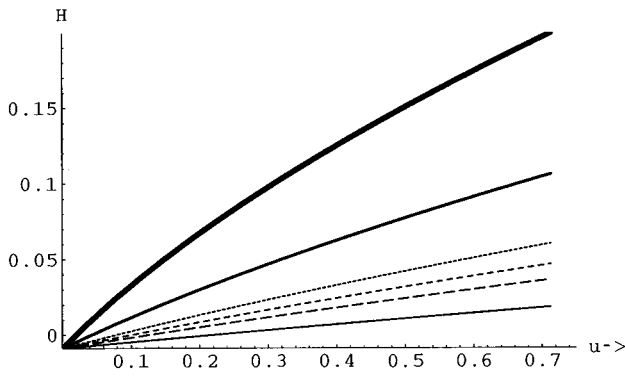
In the present work, by convoluting the event rate with the LSP velocity distribution we were able to obtain the an-



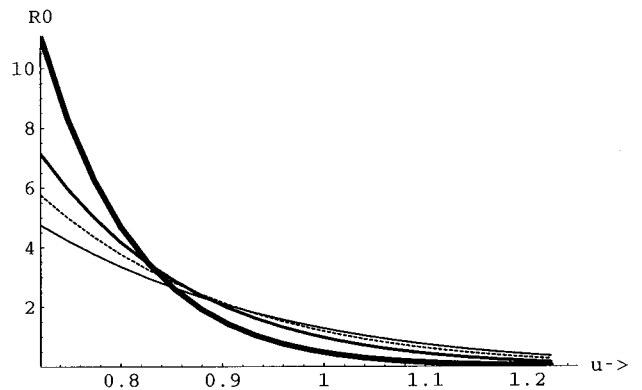
(a)



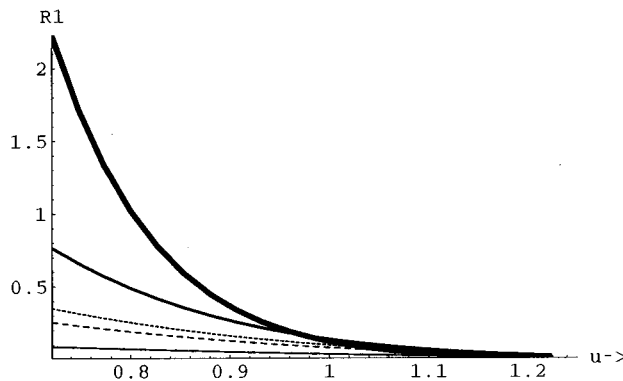
(b)



(c)



(d)



(e)

FIG. 3. The same as in Fig. 1 for the target ${}_{53}^{127}\text{I}$. (a) $R0$ for $Q_{min}=0$. (b) $R1$ for $Q_{min}=0$. (c) H for $Q_{min}=0$. (d) The same as (a) for $Q_{min}=45$ keV. (e) The same as (b) for $Q_{min}=45$ keV. The style of the curves is the same as in Fig. 1.

nual modulation effect, both for the coherent and the spin contributions, including the velocity dependence of the cross-section. We were not concerned with diurnal modulation since it is undetectable. This was done both in the total rate and in the differential rate with respect to the energy transferred to the nucleus. For the total rate we found it convenient to write our formalism in terms of three factors [see

Eq. (47)]. The first one, \bar{R} , depends on all the relevant SUSY parameters. It represents the total event rate, when the velocity dependence of the cross-section and the convolution are neglected. The second, t^0 , is the modification of the event rate due to the velocity dependence of the cross-section and the procedure of folding with the LSP velocity. The third is the modulation amplitude h . If one considers separately each

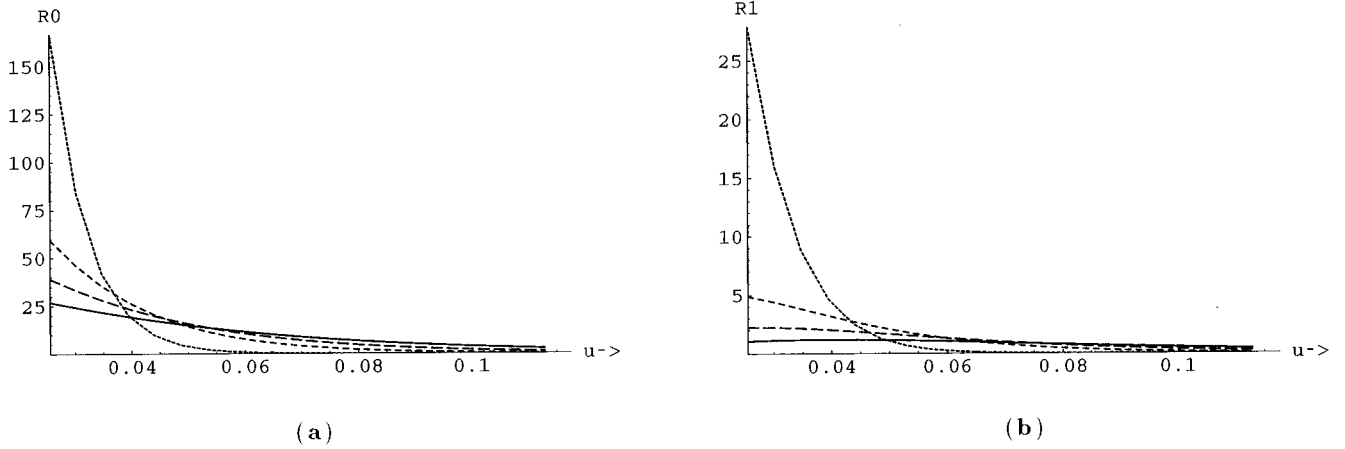


FIG. 4. The same as in Fig. 1 for the target ${}_{13}\text{Na}^{23}$. The curves shown correspond to LSP masses as follows: (i) Dotted line $\Leftrightarrow m_\chi = 10$ GeV. (ii) Dashed line $\Leftrightarrow m_\chi = 20$ GeV. (iii) Long dashed line $\Leftrightarrow m_\chi = 30$ GeV. (iv) Fine solid line $\Leftrightarrow m_\chi = 50$ GeV. For LSP masses heavier than 50 GeV the curves cannot be distinguished from (iv). (a) R_0 for $Q_{min} = 16$ keV. (b) R_1 for $Q_{min} = 16$ keV.

mode (scalar, spin, vector coherent, etc.), t^0 and h depend only on the LSP mass, the nuclear form factors and Q_{min} . The parameter t^0 for various LSP masses and a number of nuclear systems as a function of various detector energy cut-

offs is shown in Tables Ia and IIa. The total modulation amplitude h is shown in Tables Ib and IIb. We see that, even if the form factor effects are included, it is possible to have a modulation effect which is larger than the typical value, h

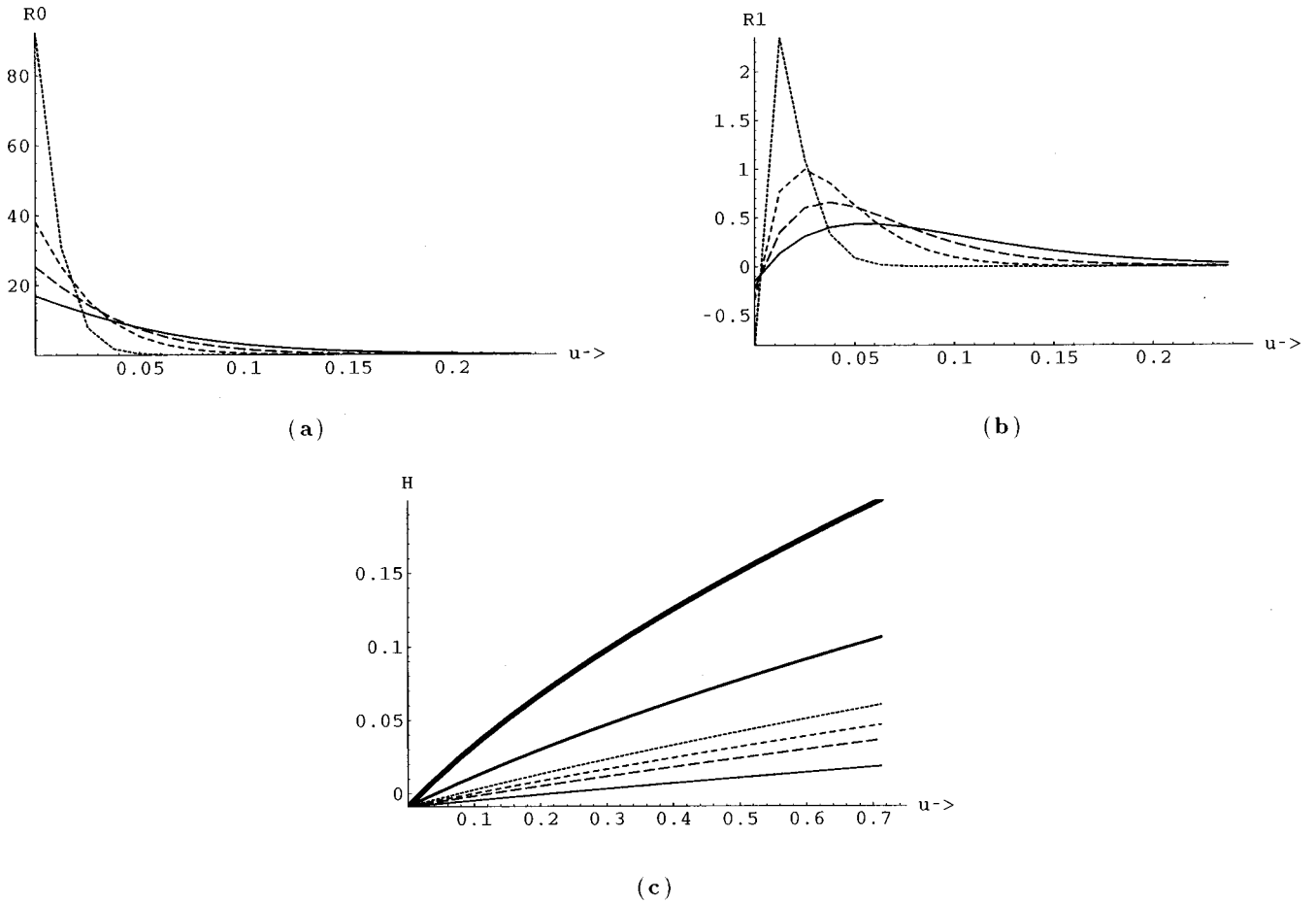


FIG. 5. The same as in Fig. 1 for the target ${}_{13}\text{Al}^{27}$ and $Q_{min} = 0.5$ keV. (a), (b) and (c) refer to R_0 , R_1 and H respectively. The style of the curves is the same as in Fig. 3.

$\leq 5\%$, but in those cases when the total rate is suppressed, e.g. for relatively small LSP mass and large Q_{min} . So detectors with large cutoffs should not be offhand considered to be disadvantaged provided that the total event rate is detectable.

In the case of the differential rate, in addition to the factors \bar{R} and t^0 mentioned above one needs two more factors [see Eq. (44)]: the relative differential rate $R0$, i.e. the differential rate divided by the total rate, and the differential modulation amplitude H . If one considers separately each mode, H depends only on the energy transfer and the LSP and target masses. The differential modulated rate $R1$ depends in addition on the nuclear form factors. It is negative at small momentum transfer and becomes positive as the momentum transfer increases. As a result h is always less than 5% [5] and tends to decrease for heavy nuclei and large LSP mass. In the case of $Q_{min}=0$ this happens because the contributions from different regions of the momentum transfer tend to cancel.

Our main result is that, even if the velocity dependence of the cross-section is incorporated into the calculation, the differential modulation amplitude H can become quite large as the momentum transfer increases [see Figs. 1(c), 3(c), and 5(c)]. Our results are encouraging, albeit less so compared to the earlier results [12,11], which disregarded the velocity de-

pendence of the cross-section. Whether such nice features can, however, be fully utilized by the experimentalists will depend on whether they can exploit the energy windows around the maximum of $R1$ shown in Figs. 1(b), 1(e), 1(g), 1(i), 3(b), 3(e), 4(b) and 5(b). The vector coherent contribution, considered by us for the first time [see Figs. 1(h)–1(j)], shows even better features, but unfortunately it may not be utilized, since the total rate \bar{R} associated with it is suppressed due to the Majorana nature of the LSP.

In conclusion we found many circumstances such that the modulation effect, both in the total as well as in the differential event rate, may aid the experimentalists in discriminating against background.

ACKNOWLEDGMENTS

The author would like to acknowledge partial support of this work by IINENΔ 1895/95 of the Greek Secretariat for research, TMR Nos ERB FMAX-CT96-0090 and ERBCHRXCT93-0323 of the European Union and the Bartol Research Foundation where most of the work was done. He would like also to thank Dr. S. Pittel and Dr. Q. Shafi for their hospitality and useful discussions. Special thanks to Dr. T. S. Kosmas for his help in preparing the manuscript.

-
- [1] For a recent review see e.g. G. Jungman *et al.*, Phys. Rep. **267**, 195 (1996).
- [2] G. F. Smoot *et al.*, Astrophys. J. **396**, L1 (1992) (COBE data).
- [3] MACHO Collaboration, D. P. Bennett *et al.*, in Proceedings of the 5th Annual Maryland Conference, 1995, edited by S. Holt (unpublished); MACHO Collaboration, C. Alcock *et al.*, Phys. Rev. Lett. **74**, 2967 (1995).
- [4] J. D. Vergados, J. Phys. G **22**, 253 (1996).
- [5] T. S. Kosmas and J. D. Vergados, Phys. Rev. D **55**, 1752 (1997).
- [6] M. Drees and M. M. Nojiri, Phys. Rev. D **48**, 3843 (1993); **47**, 4226 (1993).
- [7] M. T. Ressel *et al.*, Phys. Rev. D **48**, 5519 (1993); M. T. Ressel and D. J. Dean, Phys. Rev. C **56**, 535 (1997).
- [8] V. I. Dimitrov, J. Engel and S. Pittel, Phys. Rev. D **51**, R291 (1995).
- [9] J. Engel, Phys. Lett. B **264**, 114 (1991).
- [10] M. A. Nikolaev and H. V. Klapdor-Kleingrothaus, Z. Phys. A **345**, 373 (1993); Phys. Lett. B **329**, 5 (1993); Phys. Rev. D **50**, 7128 (1995).
- [11] A. K. Drukier *et al.*, Phys. Rev. D **33**, 12 (1986); J. I. Collar *et al.*, Phys. Lett. B **275**, 181 (1992).
- [12] P. F. Smith and J. D. Lewin, Phys. Rep. **187**, 203 (1990).
- [13] J. R. Primack, D. Seckel and B. Sadoulet, Annu. Rev. Nucl. Part. Sci. **38**, 751 (1988); F. von Feilitzch, in Proceedings of the International Workshop on Neutrino Telescopes, Venezia, 1990, edited by Milla Baldo Ceolin (unpublished), p. 257.
- [14] R. Bernabei *et al.*, Phys. Lett. B **389**, 757 (1996).
- [15] M. W. Goodman and E. Witten, Phys. Rev. D **31**, 3059 (1985); K. Griest, Phys. Rev. Lett. **62**, 666 (1988); Phys. Rev. D **38**, 2357 (1988); **39**, 3802 (1989); J. Ellis and R. A. Flores, Phys. Lett. B **263**, 259 (1991); **300**, 175 (1993); Nucl. Phys. **B400**, 25 (1993); J. Ellis and L. Roszkowski, Phys. Lett. B **283**, 252 (1992).
- [16] A. Bottino *et al.*, Mod. Phys. Lett. A **7**, 733 (1992); Phys. Lett. B **265**, 57 (1991); **402**, 113 (1997); **423**, 109 (1998); J. Edsjo and P. Gondolo, Phys. Rev. D **56**, 1789 (1997); Z. Berezhinsky *et al.*, Astropart. Phys. **5**, 1 (1996); V. A. Bednyakov, H. V. Klapdor-Kleingrothaus and S. G. Kovalenko, Phys. Lett. B **329**, 5 (1994).
- [17] G. L. Kane *et al.*, Phys. Rev. D **49**, 6173 (1994); D. J. Castaño, E. J. Piard and P. Ramond, *ibid.* **49**, 4882 (1994); D. J. Castaño (private communication); A. H. Chamseddine, R. Arnowitt and P. Nath, Phys. Rev. Lett. **49**, 970 (1982); P. Nath, R. Arnowitt and A. H. Chamseddine, Nucl. Phys. **B227**, 121 (1983); R. Arnowitt and P. Nath, Mod. Phys. Lett. A **10**, 1215 (1995); Phys. Rev. Lett. **74**, 4952 (1995); Phys. Rev. D **54**, 2394 (1996).
- [18] L. Arnowitt, in *Proceedings of the International Workshop on Non-accelerator New Physics*, Dubna, 1997 [Phys. At. Nucl. (in press)]; P. Nath and R. Arnowitt, Phys. Rev. D **56**, 2820 (1997); S. K. Soni and H. A. Weldon, Phys. Lett. **126B**, 215 (1983); V. S. Kapunovsky and J. Louis, Phys. Lett. B **306**, 268 (1993); M. Drees, *ibid.* **181**, 279 (1986); P. Nath and R. Arnowitt, Phys. Rev. D **39**, 279 (1989); J. S. Hagelin and S. Kelly, Nucl. Phys. **B342**, 95 (1990); Y. Kamamura, H. Murayama and M. Yamaguchi, Phys. Lett. B **324**, 52 (1994); S. Dimopoulos and H. Georgi, Nucl. Phys. **B206**, 387 (1981).

- [19] T. S. Kosmas and J. D. Vergados, in *Proceedings of the International Workshop on Non-accelerator New Physics* [18].
- [20] A. Wodecki, T. S. Kosmas and J. D. Vergados (in preparation).
- [21] R. Bernabei *et al.*, “Strategies to search for WIMP annual modulation signature with large-mass low radioactivity NaI(Tl) set up,” Report No. ROM2F-97-33, astro-ph/9710290; R. Bernabei *et al.*, Phys. Lett. B **389**, 757 (1996).
- [22] T. S. Kosmas and J. D. Vergados, Nucl. Phys. **A510**, 64 (1990).
- [23] R. M. Lombard *et al.*, Nucl. Phys. **101**, 601 (1967).